Biaxially Oriented Lamellar Morphology Formed by the Confined Crystallization of Poly(1,4-butylene succinate) in the Oriented Blend with Poly(vinylidene fluoride)

Yongjin Li, Akira Kaito,* and Shin Horiuchi

Research Center of Macromolecular Technology, National Institute of Advanced Industrial Science and Technology (AIST), AIST Tokyo Waterfront, 2-41-6 Aomi, Koutou-Ku, Tokyo 135-0064, Japan

Received October 6, 2003; Revised Manuscript Received January 14, 2004

ABSTRACT: The oriented crystallization of poly(1,4-butylene succinate) (PBSU) in the oriented blend with poly(vinylidene fluoride) (PVDF) was investigated at various temperatures. Films of the miscible blend with a composition of PBSU/PVDF = 30/70 (wt %) were prepared by solution casting and were subsequently quenched in ice water from the molten state. Oriented films of the blend were prepared by uniaxially stretching the melt-quenched films. The drawn films were heat-treated with the length of the sample fixed at 130 °C for 5 min to melt the PBSU component, followed by quenching in ice water or isothermal crystallization at various temperatures. The crystal orientation and the lamellar textures of the obtained samples were studied using wide-angle X-ray diffraction (WAXD), small-angle X-ray scattering (SAXS), and transmission electron microscopy (TEM). The orientation of PBSU crystals was found to be significantly dependent on the crystallization temperature when PBSU was crystallized in the oriented matrix of PVDF. When the sample was crystallized at a temperature below 30 °C, the *c* axis of PBSU crystals was parallel to the stretching direction. In contrast, the crystal *b* axis of PBSU was found to orient parallel to the stretching direction at a crystallization temperature higher than 60 °C, and thus the samples that crystallized at higher temperatures were biaxially oriented. The stretched samples displayed very strong equatorial scatterings with a long period of about 50 nm. The equatorial scattering was attributed to the periodic arrangement of PBSU-rich domains in the PVDF-rich matrix. It is considered that the morphology of the miscible blend is segregated into the fibrillar morphologies of PBSU and PVDF, forming a periodic structure with a long period of 50 nm perpendicular to the stretching direction. The TEM studies revealed that PBSU-rich domains dispersed in the PVDF-rich matrix were elongated into ribbon like domains with a width of 20−50 nm, which was consistent with the SAXS and WAXD results. On the basis of the morphologies of the blend, it was deduced that the confinement of the crystallization of PBSU within the ribbonlike domains results in the unique biaxial orientation textures. The effect of these unique orientation textures on the mechanical properties was also studied. It was found that the tensile strength of the biaxially oriented samples was higher than that of the as-drawn sample in the perpendicular direction.

Introduction

The macroscopic properties of multicomponent and multiphase polymer systems largely depend on their microscopic morphology, which includes the phase structure, the nature of the interface between phases, and the orientation of molecular chains. Therefore, controlling the morphology becomes the key to manipulating the properties of such systems. Over the past several decades, polymer blends have been of interest for microstructure control because the blending of polymers is a simple and economical method of producing new materials. Recently, oriented crystallization of polymer blends with crystallizable components has been one of the attractive procedures for microstructure control, because it may lead to the development of new superstructures in the polymer blend systems. Prud'homme et al. have studied the crystallization and orientation behaviors of poly(ϵ-caprolactone) (PCL) in the miscible blend with PCL/poly(vinyl chloride) (PVC)[1,2] and reported that the orientation of PCL depends on the conditions of crystallization and strain. We have examined the oriented crystallization of isotactic polystyrene (iPS)/poly(phenylene oxide) (PPO) blend and produced unique orientation textures containing highly oriented iPS crystals and nearly isotropic PPO chains.[3] A number of studies have been reported on the oriented crystallization of immiscible polymer blends consisting of two crystalline polymers, such as polypropylene (PP)/polyethylene (PE),[4−6] PP/isotactic poly(butene-1),[7] PP/nylon-11,[8] poly(ethylene glycol) (PEG)/nylon,[9] and polycaprolactone (PCL)/PE.[10] We have recently reported the orientation and crystallization behaviors of poly(vinylidene fluoride) (PVDF) in the oriented blends with nylon-11,[11,12] for which the specific interaction between the two components was evidenced by Fourier transform infrared (FTIR) spectroscopy. If a component with lower melting temperature is crystallized in the oriented matrix of the blends, some unusual orientation textures of dispersed phase are induced. The unique orientation behaviors have been explained on the basis of either thermal shrinkage stress,[4−6] epitaxial crystal growth on the polymer crystal,[8−10] or trans-crystallization.[7,11,12] The lack of miscibility at the interface of the two components, however, limits the improvement of the mechanical properties for the immiscible blend systems.

In this work, we try to apply the oriented crystallization to the miscible polymer blend containing two crystalline polymers. Although there have been fewer reports on the miscible crystalline/crystalline polymer blends than on the amorphous/amorphous and amorphous/crystalline polymer blends, it is expected that the

* Corresponding author. Telephone: +81-3-3599-8307. Fax: +81-3-3599-8166. E-mail: a-kaito@aist.go.jp.

10.1021/ma0355047 CCC: $27.50
Published on Web 02/24/2004

microstruture control of the crystalline/crystalline polymer blends will result in the formation of new types of superstructure. The miscibility of poly(ethylene oxide) (PEO)/poly(3-hydroxybutyrate) (PHB)[13] and PHB/poly-(L-lactide)[14] has been previously reported. Manley et al. have recently reported the miscibility, phase behaviors, crystallization kinetics, and lamellar morphologies of a miscible crystalline/crystalline blend, PVDF/poly(1,4-butylene adipate) (PBA).[15−19] More recently, Nishi et al. have studied the miscibility, crystallization kinetics, and spherulites morphology of crystalline/crystalline blends such as poly(1,4-butylene succinate) (PBSU)/PVDF,[20] poly(vinylidene chloride-*co*-vinyl chloride) (PVDCVC)/PBSU,[21−23] and poly(ethylene succinate) (PES)/PEO.[24] They investigated the interpenetrated spherulites for PBSU/PVDCVC and PES/PEO blends by optical microscopy and atomic force microscopy. In this work, a miscible crystalline/crystalline blend, PBSU/PVDF, was selected for the study of oriented crystallization. PBSU, a component with a lower melting temperature than PVDF, was crystallized in the confined domains of the oriented blend with PVDF, aiming at controlling the crystal orientation of the two components separately and thereby producing a new oriented structure, in which the two components are segregated in the nanosized domains and are oriented in different directions.

Experimental Section

Materials and Sample Preparation. PBSU and PVDF samples used in this work were purchased from Aldrich Chemical Co. Inc. and Scientific Polymer Products Inc., respectively. The PBSU/PVDF blends with a weight ratio of 30/70 were prepared by casting *N*,*N*-dimethylformamide (DMF) solution with a concentration of 3%. The cast films were dried at 100 °C under vacuum for 2 days to remove the solvent. The blends were then hot pressed at 185 °C to a film with a thickness of 200 μm, followed by rapid quenching in ice water. Oriented samples were prepared by uniaxial stretching of the molded film to a draw ratio of 4 at 80 °C with a stretching speed of 10 mm/min. The drawn samples were heat treated under strain at 130 °C for 5 min to melt the PBSU crystals, and then quickly moved to a hot stage at the desired temperature to isothermally crystallize PBSU. The isothermal process at each crystallization temperature is longer than the time required for the crystallization of PBSU in order to ensure that all the crystals are formed during the isothermal process at the designated temperature.

Characterization. Differential scanning calorimetry (DSC) was carried out under nitrogen flow at a heating rate of 10 K/min with a Perkin-Elmer DSC-7 differential scanning calorimeter calibrated with the melting temperatures of indium and zinc.

Wide-angle X-ray diffraction (WAXD) patterns were obtained by Cu Kα radiation (40 kV, 300 mA) generated by an X-ray diffractometer (Rigaku, Rint 2500 VH/PC) and an imaging plate detector. Small-angle X-ray scattering (SAXS) patterns were obtained by microfocused Cu Kα radiation (45 kV, 60 mA) generated by an X-ray diffractometer (Rigaku, Ultrax 4153A 172B) and an imaging plate detector. A hot stage (Mettler Toledo FP82HT) was used to measure the SAXS at higher temperatures.

A transmission electron microscopy (TEM) image was obtained at an acceleration voltage of 200 kV using a LEO922 (LEO Electronenmikroskopie GmbH, Oberkochen, Germany) transmission electron microscope. The oriented samples were cut into thin sections parallel to the stretching direction. The sections with thickness less than 50 nm were collected into a 600 mesh cupper grid and were served for the TEM measurement. Prior to the sectioning, embedded sample with a smooth microtomed surface was stained with RuO_4 vapor for 24 h.

Tensile tests were carried out at a rate of 2 mm/min at 20 °C and 50% relative humidity, using a tensile testing machine, Tensilon UMT-300 (Orientec Co., Ltd.). Measurements were carried out both in the stretching direction and in the direction perpendicular to it. Rectangle-shaped specimens of 2 mm width and 20 mm length were cut from the sample in the two directions, and were used for the measurements.

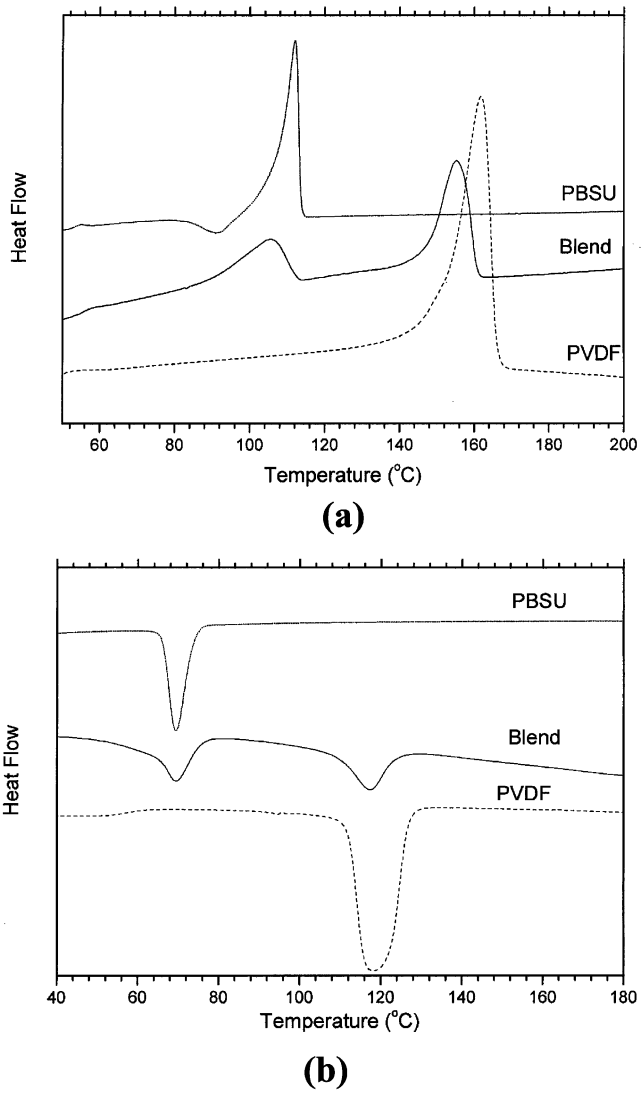

Figure 1. DSC curves of PVDF, PBSU, and PBSU/PVDF blend: (a) melting endotherms; (b) crystallization exotherms.

Results

Thermal Properties. The PBSU/PVDF blend is reported to be a miscible crystalline/ crystalline blend due to the marked decrease in melting temperature upon blending of the two components.[20] DSC curves of PBSU, PVDF, and PBSU/PVDF blend during the melting and crystallization process are shown in Figure 1. Two specific melting and crystallization peaks are observed for the blend system, indicating that PBSU and PVDF melt and crystallize separately in the blends. Melting temperatures of pure PBSU and PVDF are 115 and 160 °C, respectively, but are changed to 105 and 156 °C, respectively, in the PBSU/PVDF (30/70) blend. The melting temperatures of PBSU and PVDF markedly decrease in the blends, indicating that the blend of PBSU and PVDF is a miscible system, as reported by Nishi et al.[20] It is also observed that PBSU crystals are completely melted at 130 °C, but PVDF crystals are preserved at this temperature. Therefore, 130 °C is

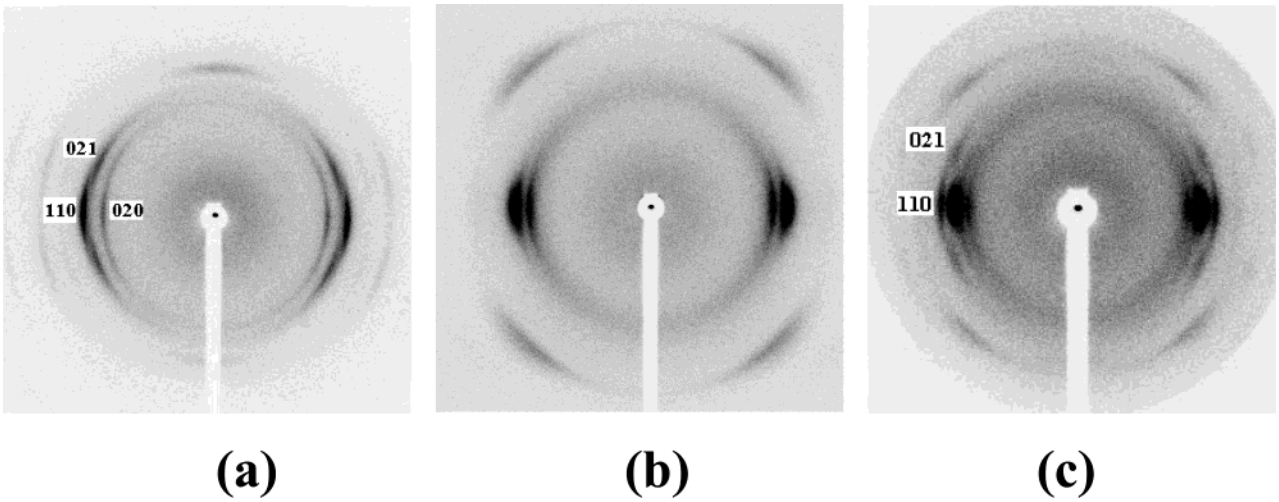

Figure 2. WAXD patterns of as-drawn samples: (a) PBSU; (b) PVDF; (c) PBSU/PVDF blend.

selected to be the heat-treatment temperature to melt PBSU in the following experiments.

Crystal Orientation. Figure 2 shows the WAXD patterns of drawn films of PVDF, PBSU, and PBSU/PVDF blend, which indicate the high degree of crystal orientation for the drawn films of PVDF, PBSU, and PBSU/PVDF blend. The WAXD pattern of PVDF shows that α and β crystalline forms coexist in the oriented sample. The former exhibits the characteristic (100) and (020) reflections at $2\theta = 17.6°$ and $2\theta = 18.8°$, respectively, on the equator, whereas the latter shows the (110)/(200) reflections at $2\theta = 20.5°$ on the equator. The WAXD pattern of PBSU, which crystallizes in the monoclinic crystal lattice with the parameters, $a = 0.523$ nm, $b = 0.908$ nm, $c = 1.079$ nm, and $\beta = 123.87°$,[25] consists of the (020) and (110) reflections ($2\theta = 19.7°$ and 22.9°, respectively) on the equator and the (021) first layer reflection ($2\theta = 22.1°$). For the as-drawn sample of PBSU/PVDF blend, the (*hk*0) reflections of both PBSU and PVDF are observed only on the equator and the (021) reflection of PBSU is located at the first layer position similar to that of the oriented pure PBSU, which reveals the superposition of the typical fiber textures (*c* axis orientation) of the two polymers. Figure 3 gives the WAXD patterns for the oriented PBSU/PVDF blends that are isothermally crystallized at various temperatures. The crystal orientation of PBSU in the blend markedly changes with crystallization temperature, while the fiber texture of the PVDF component remains unchanged and retains the *c* axis orientation. When the sample is quickly quenched to a temperature lower than 30 °C (the sample crystallized at 0 °C is hereafter designated as the **quenched sample**) after annealed at 130 °C for 5 min, the WAXD pattern is very similar to that of the as-drawn blends (shown in Figure 2c), indicating that the crystal *c* axis of PBSU is preferentially oriented parallel to the stretching direction for the quenched sample. However, when the crystallization temperature is higher than 60 °C (the sample crystallized at 80 °C is hereafter designated as the **slowly crystallized sample**), the 020 reflection of PBSU is found to move to the meridian and the 021 reflection approaches the meridian accordingly. The WAXD pattern indicates that the *b* axis of the crystal becomes parallel to the stretching direction for the sample crystallized at higher temperatures, while the PVDF matrix retains the *c* axis orientation. The intensities of the 020 reflections of PBSU on the meridian increase with increasing crystallization temperature from 40 to 60 °C, indicating that the *b* axis orientation and the *c* axis orientation coexist for the samples crystallized at intermediate temperatures (Figure 3, parts b−e) and that the fraction of the *b* axis orientation increases with increasing crystallization temperature. Unfortunately it is difficult to determine the orientation function of PBSU crystals quantitatively because of the severe overlapping of the crystal reflections of PBSU with those of PVDF.

Figure 4 shows the DSC curves of the quenched sample and the slowly crystallized sample during heating. The DSC curves are normalized by the sample weight. The melting temperatures of PBSU are 105.8 and 104.3 °C, for the slowly crystallized sample and for the quenched sample, respectively, indicating that the lamellae are thicker for the sample crystallized at higher temperature. The degrees of crystallinity of PBSU were obtained from the heat of fusion for the quenched and slowly crystallized samples. The heat of fusion for the perfect crystals of PBSU was evaluated from the heat of fusion of a melt-crystallized film of pure PBSU whose degree of crystallinity was determined by the WAXD measurement. The degrees of crystallinity of PBSU are 48% and 44% for the slowly crystallized sample and the quenched sample, respectively. It is reasonable that crystallization at higher temperature leads to the thicker lamellae and higher crystallinity.

Lamellar Structures. Figure 5 displays the Lorentz-corrected SAXS profiles of isotropic samples of pure PVDF, pure PBSU, and PBSU/PVDF blend. The SAXS intensity was normalized by thickness and exposure time, after subtracting air scattering from the observed profiles. It shows that both PVDF and PBSU exhibit a weak scattering peak at $q = 0.6$ nm^{-1} and 0.8 nm^{-1}, corresponding to long periods $L = 10$ nm and $L = 8$ nm, respectively. On the other hand, the PBSU/PVDF (30/70) blend shows a main peak at $q = 0.32$ nm^{-1} ($L = 19.6$ nm) and a minor shoulder at $q = 0.7$ nm^{-1} ($L = 9$ nm). The scattering intensity of the blend is much higher than those of the pure polymers, indicating that the magnitude of the electron density fluctuation is significantly increased for the blend relative to the pure polymers. The SAXS long period for the main peak of the blend is approximately the sum of the long periods of the pure polymers. It was considered that the molecular chains of PBSU might be partially incorporated and crystallized between the lamellae of PVDF to form

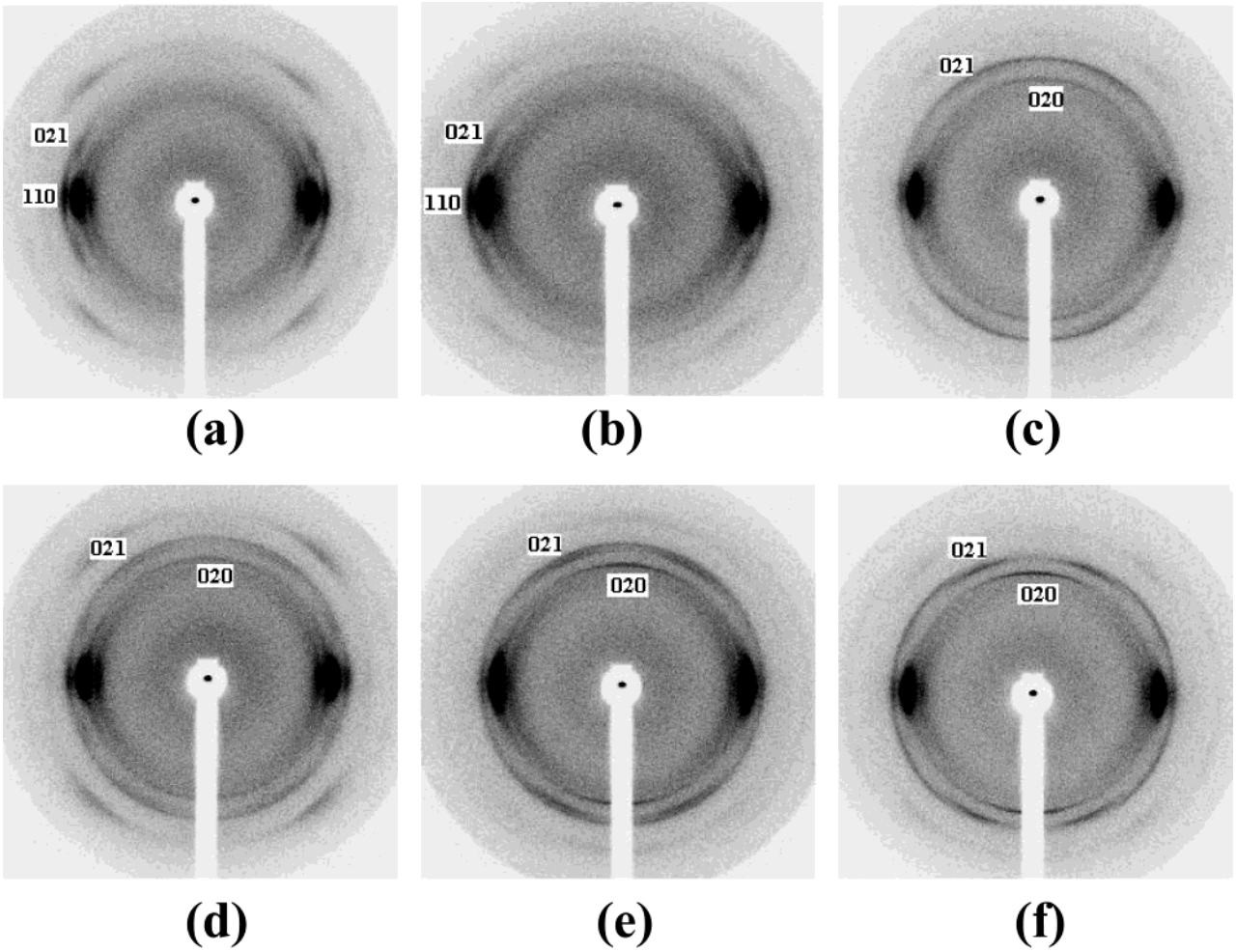

Figure 3. WAXD patterns of PBSU/PVDF blends isothermally crystallized at (a) 0, (b) 30, (c) 40, (d) 50, (e) 60, and (f) 80 °C after PBSU is melted at 130 °C.

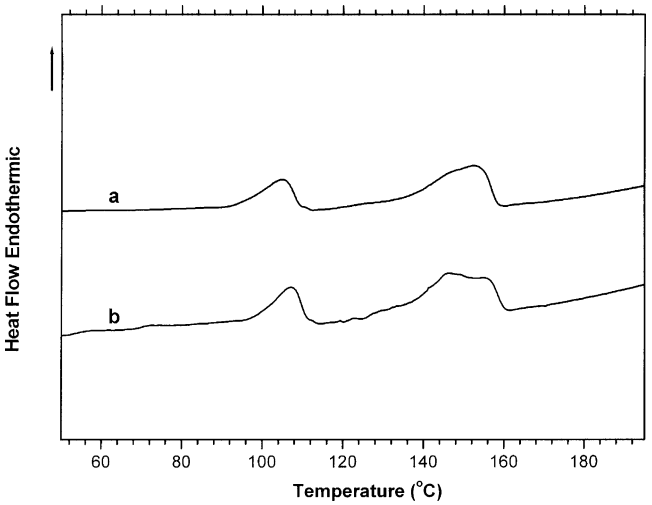

Figure 4. DSC heating diagrams of (a) quenched sample of blend and (b) a slowly crystallized sample of blend. The heating rate is 10 °C/min.

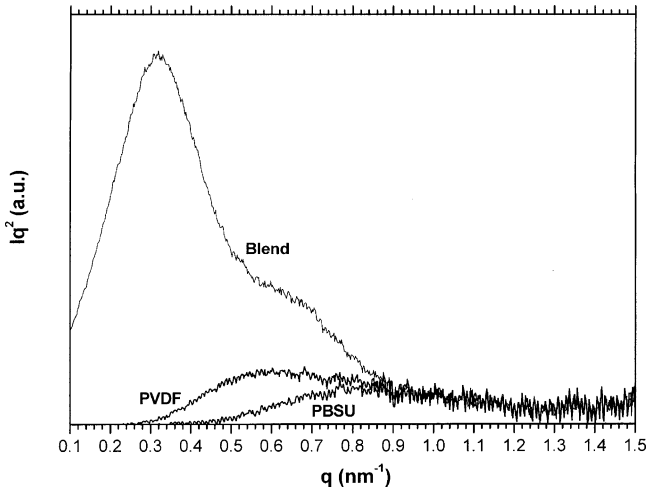

Figure 5. Lorentz-corrected SAXS profiles of isotropic samples of PVDF, PBSU, and PBSU/PVDF blend.

the interlamellar inclusion morphology. On the other hand, two possibilities are considered for the shoulder at $q = 0.7$ nm^{-1} ($L = 9$ nm). The shoulder is possibly assigned to another lamellar morphology in which the molecular chains of PBSU are excluded from the lamellar stacks of PVDF and are segregated to form its own lamellar stacks (interlamellar exclusion mode). The SAXS profile of PBSU/PVDF blend is similar to the reported SAXS profile of PVDF/PBA = 50/50 blend crystallized by a single quenching process, for which the two types of lamellar morphology coexist.[18] It is also possible to assign the two peaks to the first and the second-order peaks of the interlamellar inclusion structure. In any case, the interlamellar inclusion structure exists in the isotropic samples of PBSU/PVDF = 30/70 blend, but it is difficult to verify the presence of the

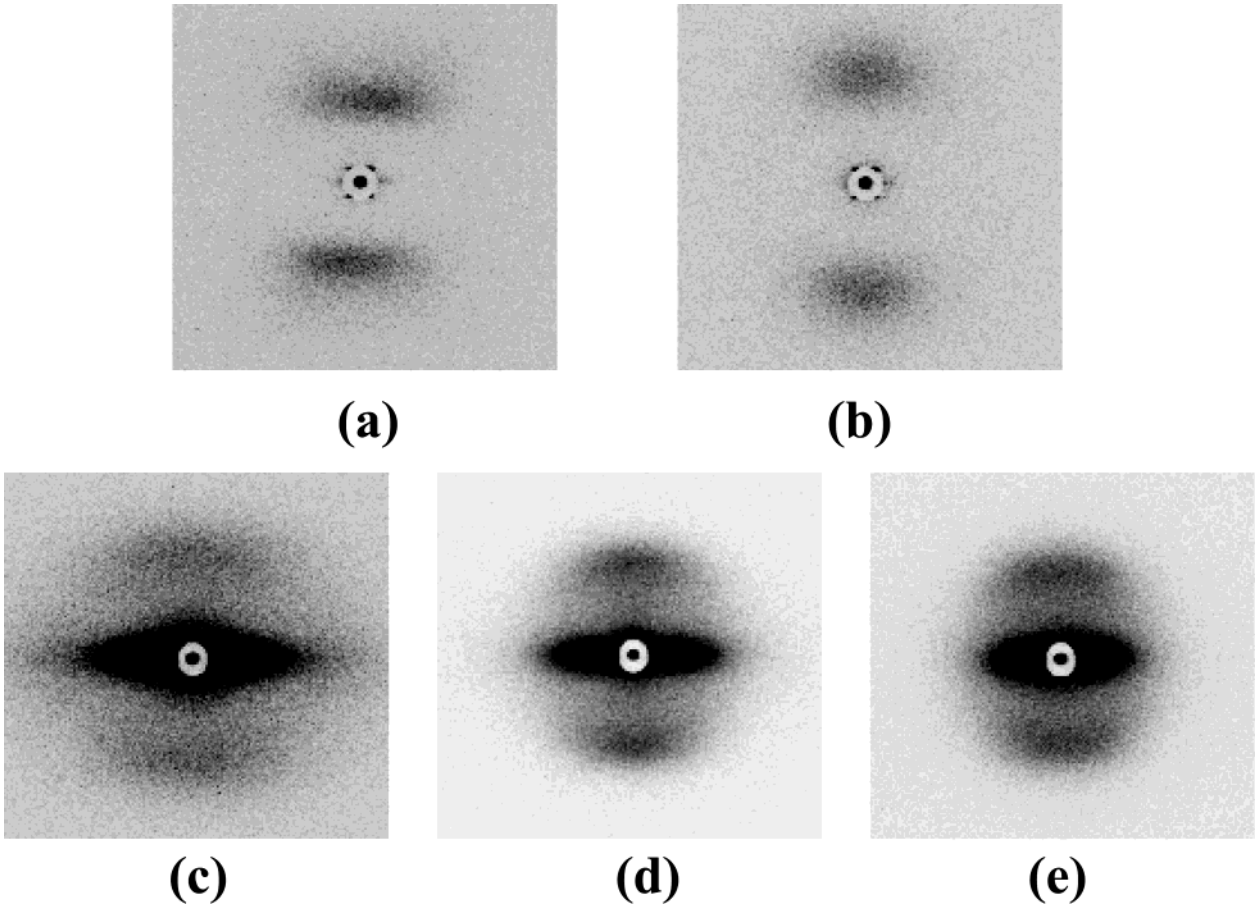

Figure 6. SAXS patterns: (a) as-drawn sample of PVDF; (b) as-drawn sample of PBSU; (c) as-drawn sample of blend; (d) quenched sample of blend; (e) slowly crystallized sample of blend.

interlamellar extrusion morphology in the isotropic blend sample.

Figure 6 shows the SAXS images for the as-drawn samples of PVDF, PBSU, and PBSU/PVDF blend, as well as those of the quenched and slowly crystallized samples of the blend. For as-drawn PVDF and PBSU, the scattering lobes are located only in the meridional direction, indicating that the lamellae are stacked along the stretching direction (Figure 6, parts a and b). For the oriented blends including the quenched and slowly crystallized samples, however, a very strong scattering can be observed in the equatorial direction in addition to the meridional lobes (Figure 6, parts c−e). The scattering in the equatorial direction indicates that large electron density fluctuation is induced perpendicular to the stretching direction and that there exist some periodic structures perpendicular to the stretching direction.

It is clear that the meridional scattering originates from the crystal lamellar structure stacked along the stretching direction. Figure 7 displays the Lorentz-corrected meridional SAXS profiles for the oriented PBSU/PVDF blends as well as for the stretched PVDF and PBSU. For the oriented blend samples, only one symmetric scattering peak can be observed in the meridian direction, which is different from the profile for the isotropic blend (Figure 5). The long period of the as-drawn blend is 8.6 nm and close to the values of the long period of the pure polymers (L = 10.3 nm and L = 8.3 nm for PVDF and PBSU, respectively). The intensity of the meridional SAXS for the as-stretched blend is also similar to that for the pure polymers, indicating that

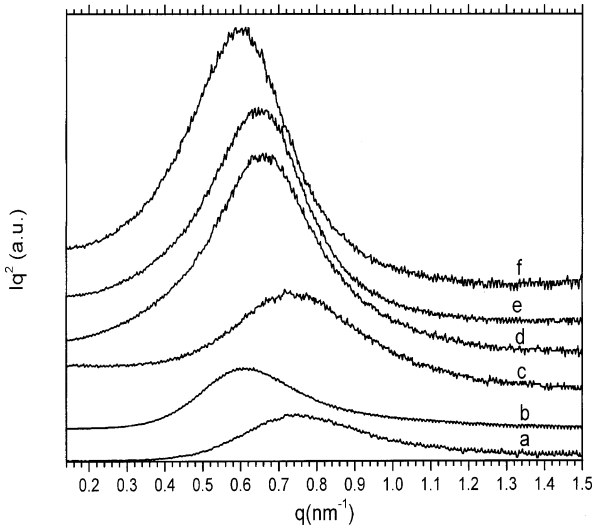

Figure 7. Lorentz-corrected SAXS profiles of oriented samples in the meridional direction: (a) as-drawn sample of PBSU measured at 25 °C; (b) as-drawn sample of PVDF measured at 25 °C; (c) as-drawn sample of PBSU/PVDF blend measured at 25 °C; (d) quenched sample of PBSU/PVDF blend measured at 25 °C; (e) slowly crystallized sample of PBSU/PVDF blend measured at 25 °C; (f) slowly crystallized sample of PBSU/PVDF blend measured at 130 °C.

only the interlamellar exclusion morphology is present for the oriented sample. The crystallites of PBSU are excluded from the lamellar stacks of PVDF and are segregated into nanosized fibrillar domains during stretching. The interlamellar exclusion morphology

might be stabilized for the oriented samples, because tie-molecules should be produced between crystallites and act as stress transmitters during stretching. The long periods of quenched and slowly crystallized samples of the blend are longer than that of the as-stretched sample. In addition, the scattering intensity of the meridional SAXS is higher for the quenched and slowly crystallized samples than that for the as-drawn sample. These results suggest the occurrence of reorganization of the periodic structure of lamellar stacks during the heat treatment, such as the thickening and ordering of the lamellae of PVDF and the partial diffusion of amorphous chains of PBSU between the lamellae of PVDF.

The meridian SAXS profiles for the quenched sample (Figure 7d) and for the slowly crystallized sample (Figure 7e) are similar to each other, although the orientation patterns of PBSU crystals are quite different from each other. The meridian scattering of the slowly crystallized sample comes only from oriented PVDF crystals, but both PVDF and PBSU lamellae contribute to the meridian scattering for the quenched sample. However, the contribution of PBSU crystal is not very large because only 30% PBSU exists in the blends and the degree of crystallinity is lower for the quenched sample than for the slowly crystallized sample. Therefore, there is not much difference in the meridian SAXS between the slowly crystallized sample and the quenched sample.

Now let us consider the equatorial scattering for the stretched blend samples. Careful discussion is required for determining the origin of the strong equatorial scattering. One might expect that the equatorial scattering may originate from some microvoiding that is induced by stretching. The strong equatorial scattering can be observed for the sample with a draw ratio as low as 2, but it is unnatural to consider the microvoid formation at a very low draw ratio. Furthermore, microvoids are not observed by transmission electron microscopy. The studies on the meridional SAXS for the stretched sample indicate that the interlamellar exclusion morphology is the dominating lamellar structure for the stretched blends. The densities of PBSU and PVDF are 1.30 and 1.80 g/cm^3, respectively, resulting in a very apparent electron density fluctuation in the blend samples. When we combine this morphology of the blend with the large density difference of PVDF and PBSU, it is reasonable to attribute the equatorial scattering to the ordered arrangement of the PBSU-rich and PVDF-rich domains in the stretched blend samples. The PBSU-rich domains are elongated in the stretching direction and dispersed in the matrix of PVDF forming a periodic density fluctuation in the direction perpendicular to the stretching direction.

The Lorentz-corrected SAXS profiles of the PBSU/PVDF blends in the equatorial direction are shown in Figure 8. They display apparent scattering peaks at the very low q-position. To obtain the long period and the correlation length, accurately, the one-dimensional correlation function ($K(r)$) is calculated by the following equation:[26]

$$K(r) = (1/2\pi^2)\int_0^{\pi} Iq^2 \cos(qr)\, \mathrm{d}q \qquad (1)$$

where $I(q)$ is the scattering intensity and r is the distance for which the electron density correlation is measured. The one-dimensional correlation functions for

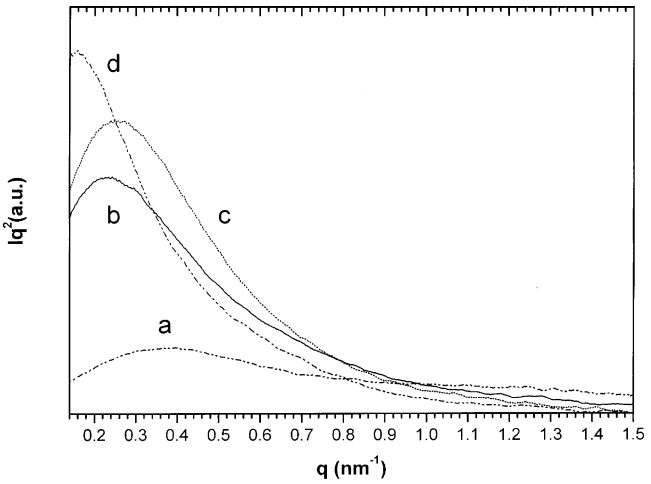

Figure 8. Lorentz-corrected SAXS profiles of PBSU/PVDF blend in the equatorial direction: (a) as-drawn sample measured at 25 °C; (b) quenched sample measured at 25 °C; (c) slowly crystallized sample measured at 25 °C; (d) slowly crystallized sample measured at 130 °C.

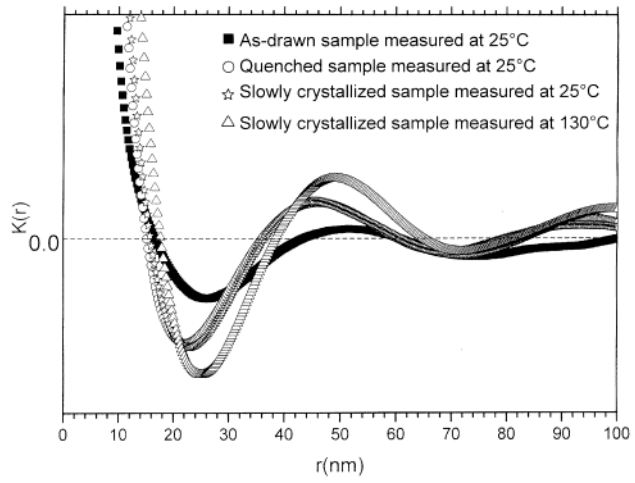

Figure 9. One-dimensional correlation functions obtained from the equatorial SAXS of the oriented blend samples.

the equatorial scattering of the oriented blends are shown in Figure 9. It is shown in the figure that the long period of the periodic structure in the equatorial direction is about 50 nm and the correlation length is 20−25 nm. The scattering intensity increases and the scattering peak shifts to the lower-q position by melting and recrystallization of PBSU, indicating that the periodic structure in the vertical direction is reorganized into the structure with longer periods during the melting and recrystallization process. In addition, the equatorial SAXS is intensified at 130 °C, where the PBSU crystal is melted (Figure 8d). The electron density difference between the PVDF-rich and PBSU-rich domains is increased at 130 °C because the density of PBSU is decreased in the molten state compared to the density of PBSU crystals.

The lamellar structures expected from the results of SAXS and WAXD are schematically shown in Figure 10. Molecular chains of PBSU are located in the nanosized domains surrounded by the fibrillar morphology rich in PVDF, when PBSU is melted at 130 °C (Figure 10a). The fibrillar morphology is retained even above the melting temperature of PBSU. PBSU crystallizes between the fibrillar morphology of PVDF, when the

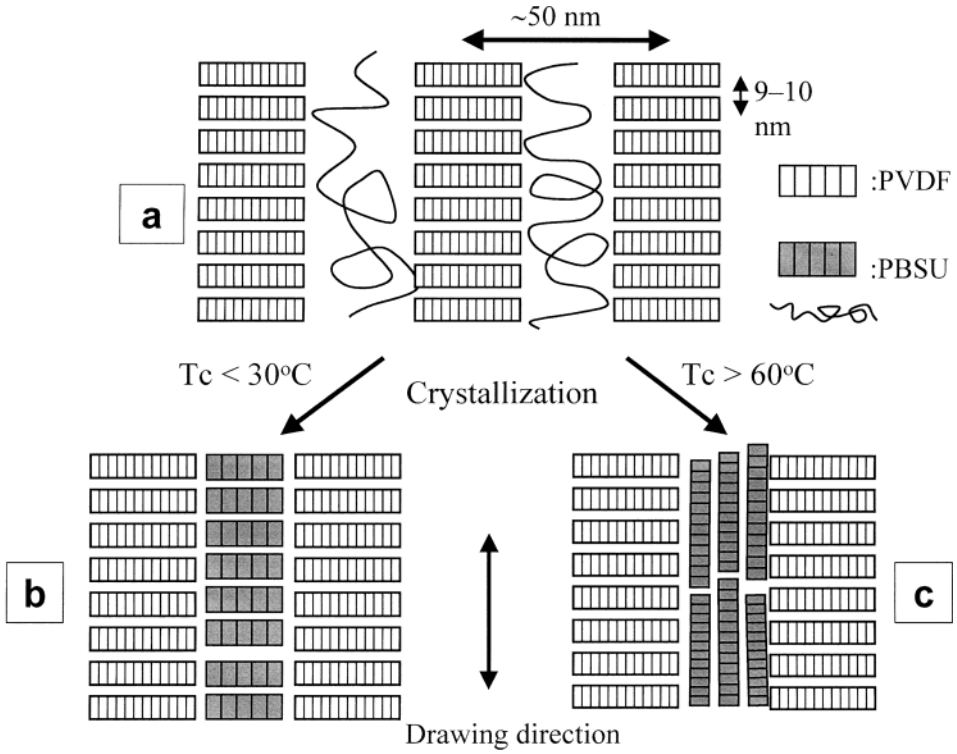

Figure 10. Schematic representation of lamellar morphologies for (a) the stretched PVDF/PBSU blends at 130 °C, (b) quenched samples, and (c) slowly crystallized samples.

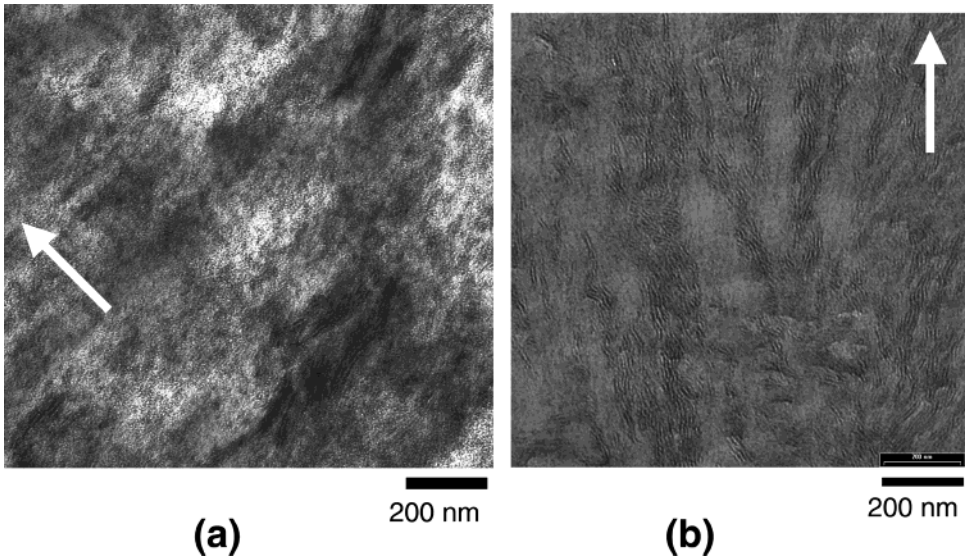

Figure 11. TEM micrographs for (a) the quenched sample and (b) the slowly crystallized sample. The arrow shows the drawing direction.

sample is quenched to the crystallization temperature. The crystallization at lower temperatures (T_c < 30 °C) results in the parallel orientation texture, in which the lamellae of PBSU are oriented in the same direction as those of PVDF (Figure 10b). On the other hand, the crystal *c* axis (molecular chain axis) of PBSU is perpendicular to the drawing direction, forming a biaxially oriented lamellar morphology, when the crystallization temperature is higher than 60 °C (Figure 10c).

Morphologies. Figure 11 shows the TEM images of the quenched sample and the slowly crystallized sample. The lamellae of PBSU for the quenched sample are perpendicular to the stretching direction (Figure 11a), but those in the slowly crystallized sample are oriented parallel to the stretching direction (Figure 11b), indicating that the molecular chain axis of PBSU in the quenched sample and the slowly crystallized sample are different, which is consistent with the results of WAXD. The lamellar morphology in the PVDF-rich domains is not identified in the TEM micrographs. The regions without lamellae are considered to be the PVDF-rich domains, which cannot be stained with RuO_4, because the strained tie-molecules are produced in the amorphous regions between the lamellae of PVDF during stretching. It is also observed in the TEM image of the slowly crystallized sample (Figure 11b) that PBSU-rich domains consist of stacks of a few lamellae and are elongated along the stretching direction, forming a ribbonlike structure with a width of 20−50 nm. The correlation length and the long period obtained from the

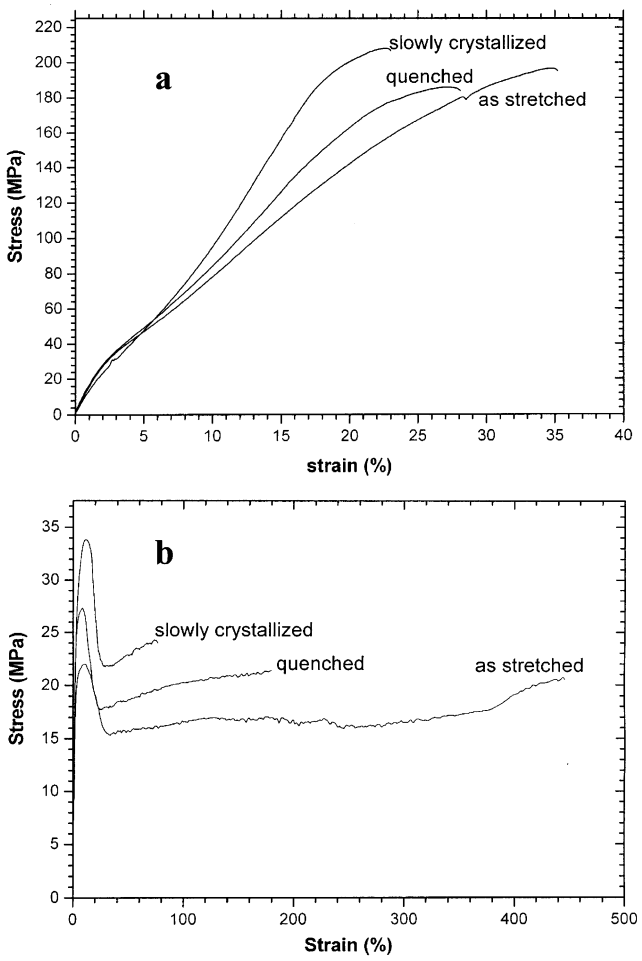

Figure 12. Stress−strain curves of the oriented PVDF/PBSU blends: (a) parallel direction; (b) perpendicular direction.

SAXS equatorial profile are 20−25 and 50 nm, respectively, which correspond to the width and the periodicity of the PBSU-rich domains, respectively. The domain structure of the PBSU-rich domains is however not clearly observed in the TEM image of the quenched sample (Figure 11a). It is considered that the TEM images are affected by the details of the staining conditions. The observed morphologies are however consistent with those expected from the results of WAXD and SAXS as a whole.

Mechanical Properties. It is very interesting to study the influence of the biaxial orientation of PVDF and PBSU on the properties of the material, particularly perpendicular to the stretching direction. Therefore, the mechanical properties are characterized both in the stretching direction and in the perpendicular direction. The results of the stress−strain curves are shown in Figure 12. The yield point is observed at very low strain in the stress−strain curve in the perpendicular direction, but samples are deformed without showing a yield point in the stretching direction. The ultimate strength of the slowly crystallized sample is similar to those of quenched and as-drawn samples in the parallel direction, and is nearly one order higher than the ultimate strength of the isotropic sample of PBSU/PVDF blend. However, the slowly crystallized sample shows much higher yield strength in the perpendicular direction than the as-drawn sample. The marked increase in strength from 22.5 to 34.2 MPa can be attributed to the perpendicular orientation of PBSU crystals and the mutual diffusion of the two polymers between the PVDF-rich and PBSU-rich domains. The molecular chains of both PBSU and PVDF are oriented in the stretching direction for the as-drawn sample, so the strength in the perpendicular direction is very low. For the slowly crystallized sample, however, the crystal *b* axis of PBSU is oriented in the stretching direction, and thereby the crystal *c* axis of PBSU will be aligned perpendicular to the stretching direction. Thus, the improvement of the strength both in the stretching direction and in the perpendicular direction originates from the biaxial orientation of PVDF and PBSU in the slowly crystallized blend sample.

Discussion

It is important to elucidate the mechanism of the formation of the unique biaxial orientation texture when the sample is crystallized at higher temperatures. To date, epitaxial crystallization,[8−10] thermal shrinkage stress,[4−6] and trans-crystallization[7,11,12] have been used to interpret some new orientation behaviors observed in some biconstituent fibers and PP/PE blend systems. Possibilities of lattice matching are not found for PBSU and PVDF crystals. Furthermore, different orientation modes are observed for our system at different crystallization temperatures. Therefore, the epitaxial crystallization of PBSU on the surface of PVDF can be ruled out. For the thermal shrinkage mechanism, it is commonly accepted that the thermal shrinkage force should be higher for the rapid quench treatment than for the slow crystallization process. The unique orientation textures would be more easily obtained for the quenched sample than for the slowly crystallized sample if thermal shrinkage accounts for the changes of the orientation modes. However, in the present case, the biaxial orientation can be obtained only when the sample is crystallized at higher temperatures. We have reported a new type of orientation texture of PVDF crystals that is crystallized in the oriented blend of PVDF/Nylon 11.[11,12] The studies show that the orientation texture comes from the trans-crystallization of PVDF at the interface of PVDF and nylon-11. However, there is no evidence that supports the occurrence of trans-crystallization in the PBSU/PVDF blend system.

Another mechanism that should be considered is the confinement of crystal growth in the nanosized domains. It was reported that the crystal orientation was induced by the confinement of crystal growth in the narrow channels formed between inorganic fibers[27,28] or the drawn polymer matrix.[29,30] The nanoconfined crystallization was also studied for the ordered block copolymers in the lamellar[31,32] and cylinder[33] morphologies. The difference in density between PBSU and PVDF results in the strong density fluctuation perpendicular to the drawing direction, which gives rise to the intense equatorial SAXS. TEM images show the unique morphology for the PBSU/PVDF blend system, which is consistent with the SAXS profiles. Lamellae of PBSU build up the ribbonlike domains, which are dispersed in the oriented matrix of PVDF. The diameter of the PBSU-rich domains is several tens of nanometers and the length is several hundreds of nanometers. It was reported that the crystal *b* axis is the axis of fastest crystal growth in the case of PBSU.[34] The WAXD shows that the *b* axis of PBSU crystals orients in the stretching direction, indicating that the crystal growth proceeds along the long axis of ribbonlike domains, which are

oriented parallel to the stretching direction. This indicates that the confinement of crystal growth is the mechanism of the unique orientation textures of PBSU crystals at higher crystallization temperatures. The molten chains of PBSU are also located in the narrow ribbonlike domains surrounded by the oriented PVDF-rich matrix when the sample is heated to 130 °C under strain. When PBSU is slowly crystallized at higher temperatures, the crystals have to grow along the long axis of the ribbonlike domains owing to the spatial confinement in the radial direction, and thereby, the crystal growth of PBSU proceeds parallel to the stretching direction.

On the other hand, the other mechanism is effective in the case of the oriented crystallization of the quenched sample. The molecular chains of PBSU will align parallel to the oriented chains of PVDF because of the miscibility of the two polymers. If the rate of crystallization is fast, molecular chains of PBSU will crystallize with the orientation retained. To confirm this mechanism for the oriented crystallization during the quenching, we have crystallized a thin film of PBSU on the surface of the oriented PVDF by quenching the sample from 130 °C to room temperature. The polarized FTIR measurement of the sample shows that the molecular orientation is induced for PBSU due to the miscibility with the oriented PVDF film. Thus, the parallel orientation of PBSU at a lower crystallization temperature is caused by the miscibility of the two polymers, whereas the perpendicular orientation is induced by the crystallization confinement in the nanosized domains.

Conclusion

Oriented crystallization of PBSU in the oriented blend with PVDF was studied under various crystallization conditions. An intense equatorial scattering is discernible in the SAXS patterns of the stretched films of PBSU/PVDF blends and the scattering is attributed to the ordered arrangement of PBSU-rich domains in the PVDF-rich matrix in the oriented blend samples. It is considered that the morphology of the miscible PBSU/PVDF blend is segregated into the fibrillar morphology of the components, forming a periodic structure with a long period of about 50 nm perpendicular to the stretching direction. When we recrystallize PBSU in the nanosized domains after melting PBSU crystals between the melting temperatures of the two polymers, the orientation textures of PBSU are dependent on the crystallization conditions. When the sample is crystallized below 30 °C, the *c* axis of PBSU crystals is parallel to the stretching direction. In contrast, the crystal *b* axis is found to orient parallel to the stretching direction at a crystallization temperature higher than 60 °C. The *c* axis orientation of PBSU at lower crystallization temperatures is caused by the miscibility of the two polymers, whereas the *b* axis orientation is induced by the crystallization confinement in the nanosized domains. The biaxial orientation of PVDF and PBSU is a new type of morphology of polymeric systems, in which the crystallites of the two polymers are oriented in mutually opposite direction, crystalline domains of the two polymers are dispersed on the scale of tens of nanometers, and the molecular chains of the two polymers are miscible in the amorphous phase. The tensile strength of the biaxially oriented sample is higher in the perpendicular direction than that of the as-drawn sample of PBSU/PVDF blend. The biaxial orientation of the blend sample is considered to be responsible for the improvement of tensile properties.

Acknowledgment. Y.L. would like to thank the Japan Society for the Promotion of Science (JSPS) for providing the fellowship and Grant-in-Aid PB01090 to do this research at National Institute of Advanced Industrial Science and Technology (AIST). This study is carried out as "Nanostructure Polymer Project" supported in part by NEDO (New Energy and Industrial Technology Development Organization) launched in 2001. The authors thank the reviewers for valuable suggestions.

References and Notes

(1) Zhao, Y.; Keroack, D.; Prud'homme, R. *Macromolecules* **1999**, *32*, 1218.
(2) Morin, D.; Zhao, Y.; Prud'homme, R. *J. Appl. Polym. Sci.* **2001**, *81*, 1683.
(3) Dikshit, A.; Kaito, A. *Polymer* **2003**, *44*, 6647.
(4) Nishio, Y.; Yamane, T.; Takahashi, T. *J. Macromol. Sci.—Phys.* **1984**, *B23*, 17.
(5) Kojima, M.; Satake, H. *J. Polym. Sci. Polym Phys.* **1984**, *22*, 285.
(6) Gross, B.; Petermanm, J. *J. Mater. Sci.* **1984**, *19*, 105.
(7) Takahashi, T.; Nishio, Y.; Mizuno, H. *J. Appl. Polym. Sci.* **1987**, *34*, 2757.
(8) Seth, K. K.; Kempster, C. J. E. *J. Polym. Sci., Polym. Symp.* **1977**, *58*, 297.
(9) Fornes, R. E.; Grady, P. L.; Hersh, S. P.; Bhat, G. R.*J. Polym. Sci., Polym. Phys.* **1976**, *14*, 559.
(10) Takahashi, T.; Inamura, M.; Tsujimoto, I. *Polym. Lett.* **1970**, *8*, 651.
(11) Li, Y. J.; Kaito, A. *Macromol. Rapid Commun.* **2003,** *24*, 255.
(12) Li, Y. J.; Kaito, A. *Macromol. Rapid Commun.* **2003**, *24*, 603.
(13) Avella, M.; Martuscelli, E. *Polymer* **1988**, *29*, 1731.
(14) Blumm, E.; Owen, A. J. *Polymer* **1995**, *36*, 4077.
(15) Penning, J. P.; Manley, R. St. J. *Macromolecules* **1996**, *29*, 77.
(16) Penning, J. P.; Manley, R. St. J. *Macromolecules* **1996**, *29*, 84.
(17) Fujita, K.; Kyu, T.; Manley, R. St. J. *Macromolecules* **1996**, *29*, 91.
(18) Liu, L. Z.; Chu, B.; Penning, J. P.; Manley, R. St. J. *Macromolecules* **1997**, *30*, 4398.
(19) Liu, L. Z.; Chu, B.; Penning, J. P.; Manley, R. St. J. *J. Polym. Sci., Part B: Polym. Phys.* **2000**, *38*, 2296.
(20) Lee, J. C.; Tazawa, H.; Ikehara, T.; Nishi, T. *Polym. J.* **1998**, *30*, 327.
(21) Lee, J. C.; Tazawa, H.; Ikehara, T.; Nishi, T. *Polym. J.* **1998**, *30*, 780.
(22) Terada, Y.; Ikehara, T.; Nishi, T. *Polym. J.* **2000**, *32*, 900.
(23) Hirano, S.; Terada, Y.; Ikehara, T.; Nishi, T. *Polym. J.* **2001**, *33*, 371.
(24) Qiu, Z.; Ikehara, T.; Nishi, T. *Macromolecules* **2002**, *35*, 8251.
(25) Ueda, A. S.; Chatani, Y.; Tadokoro, H. *Polym. J.* **1971**, *2*, 387.
(26) Strobl, G. R.; Schneider, M. *J. Polym. Sci., Part B: Polym. Phys.* **1980**, *18*, 1343.
(27) Lhymn, C.; Schultz, J. M. *Polym. Compos.* **1985**, *6*, 87.
(28) Waddon, A. J.; Hill, M. J.; Keller, A.; Blundell, D. J. *J. Mater. Sci.* **1987**, *22*, 1773.
(29) Mencik, Z.; Plummer, H. K.; Oene, H. V. *J. Polym. Sci., Part A-2* **1972**, *10*, 507.
(30) Schultz, J. M. *J. Polym. Sci., Part B: Polym. Phys.* **1992**, *30*, 785.
(31) Hamley, I. W.; Fairclough, J. P. A.; Terrill, N. J.; Ryan, A. J.; Lipic, P. M.; Bates, F. S.; Towns-Andrews, E. *Macromolecules* **1996**, *29*, 8835.
(32) Zhu, L.; Calhoun, B. H.; Ge, Q.; Quirk, R. P.; Cheng, Z. D.; Thomas, E. L.; Hsiao, B. S.; Yeh, F.; Liu, L.; Lotz, B. *Macromolecules* **2001**, *34*, 1244.
(33) Huang, P.; Zhu, L.; Cheng, S. Z. D.; Ge, Q.; Quirk, R. P.; Thomas, E. L.; Lotz, B.; Hsiao, B. S.; Liu, L.; Yeh, F. *Macromolecules* **2001**, *34*, 6649.
(34) Ihn, K. J.; Yoo, E. S.; Im, S. S. *Macromolecules* **1995**, *28*, 2460.

MA0355047